Comparison of a Small Slope Approximation Model of Reflection Loss at the Rough Ocean Surface with Stochastic Modelling using PE

Adrian D. Jones (1), Amos Maggi (2), David W. Bartel (1), Alec J. Duncan (2) and Alex Zinoviev (1)

(1) Defence Science and Technology Organisation, P.O. Box 1500, Edinburgh, SA 5111, Australia
(2) Centre for Marine Science & Technology, Curtin University of Technology, GPO Box U1987, Perth WA 6845, Australia

ABSTRACT

The accurate modelling of underwater acoustic reflection from a wind-roughened ocean surface is a challenging problem. Some complicating factors are the presence of near-surface bubbles and the potential for shadowing of acoustic energy by parts of the surface itself. One essential factor, which is the subject of the present paper, is the specular reflection of coherent plane waves at an ocean-like rough surface. We tested the accuracy of the rough surface reflection model adopted by the authors, the small-slope approximation (SSA) approach as used by Williams et al. (JASA, 116, Oct. 2004). The SSA model was used to compute values of the coherent plane wave reflection loss per bounce for wind speeds between 5 and 12.5 m/s, frequencies between 1.5 and 9 kHz, and grazing angles between about 1 and 10 degrees. These values were compared to those obtained from a Monte-Carlo approach based on the Parabolic Equation (PE) method, where realistic ocean surfaces were generated based on the Pierson-Moskowitz spectrum for ocean surface heights. The SSA model compared favourably with the more rigorous PE method for most of the range of parameters considered.

INTRODUCTION

The transmission of underwater sound signals usually involves reflection from the ocean surface. Further, sound transmission to medium or long ranges in shallow oceans (in excess of about 10 km), and transmission in a surface duct, usually involves incidence at the surface at small grazing angles. When wind action or swell causes the surface to be roughened, it is well known that the amplitude of the specular reflection is reduced. This reduction occurs as some acoustic energy is scattered at non-specular angles, and under certain conditions some energy is absorbed. These events are due to a combination of the complex sea surface shape and the effects from near-surface bubbles generated by the wind. One effect of the bubbles is to increase the compressibility of the bubbly water, thereby reducing the speed of sound and causing upward refraction of the sound (see, e.g. Jones et al., 2011). Another effect of the bubbles is to cause absorption and scattering (see, e.g. Hall, 1989). This paper is, however, concerned solely with the reflection loss due to the scattering of sound from the roughened surface. The refractive effect of bubbles is considered in this work, but other effects from bubbles are ignored.

The reflection loss for sound incident at a roughened surface has received much attention over a long period of time, as is well known. Most of this has been concerned with the coherent reflection at the specular angle. There is a considerable body of literature relating to the underwater application, for which the roughened surface has the form of the sea surface. Work of the early 1960s includes that of Marsh et al. (1961). Subsequently, Kuo (1988) reported errors in the work of Marsh et al. More recently, a considerable body of work was carried out at APL-UW by Thorsos et al. (e.g. Thorsos and Broschat, 1995). An application of this work to sound incident at small grazing angles at the sea surface was reported by Williams et al. (2004). In that work, Williams et al. compared different simulations of the acoustic field for several shallow water scenarios. For one set of simulations, the Gaussian beam model GRAB was run with the APL-UW small-slope approximation model (SSA) of coherent surface reflection loss. Another set of simulations was obtained as coherent averages of the complex pressure fields obtained over (more than 50) Monte Carlo runs of a Parabolic Equation (PE) transmission code with random realisations of a roughened sea surface. A comparison of the field details at 20 km range showed very good agreement between respective sets of data for acoustic frequency 3.2 kHz and wind speeds 5 and 10 m/s. Agreement between the PE and GRAB-with-SSA surface loss modelling (Williams et al. 2004) was less for a high loss case with frequency of 6 kHz and wind speed of 10 m/s. Williams et al. believed this to be largely due to the fact that their scenario used an isovelocity sound speed profile, causing the field at 20 km range to be determined by extremely small angles of incidence, for which the high loss (2 dB loss at 1°) precluded a cancellation near the surface of the incident and reflected signals. These comparisons of Williams et al. were, nonetheless, most favourable and so the authors chose to prepare a model based on the description given (Williams et al. 2004) of the APL-UW SSA algorithm.

In order to gain confidence in the use of the SSA model described by Williams et al. (2004), the authors (Jones et al. 2010) carried out some comparisons of limited extent. These repeated the wind speed/frequency combinations of 5 and 10 m/s for 3.2 kHz as used by Williams et al. (2004). This work, however, involved the determination of loss-per-bounce values, using PE modelling, for a variety of individual grazing angles, whereas the paper of Williams et al. (2004) shows comparisons only for shallow ocean scenarios which include combined effects of reflections at many grazing angles. The present paper reports more recent work in

which the authors have made similar comparisons of loss-per-bounce from the SSA model with PE results, but for a larger spread of wind speed/frequency combinations.

The paper commences with a brief description of the APL-UW small-slope approximation model (SSA), and then describes the PE modelling technique which the authors have used to determine reflection loss per bounce. The differences between the current and previous (Jones et al. 2010) method of PE modelling that the authors have used are described briefly. Lastly, the comparisons are presented and discussed.

MODEL OF ROUGHNESS LOSS AT THE SEA SURFACE

Values of coherent reflection loss at the sea surface are usually taken to refer to incident plane waves of infinite extent. The reflection, and reflection loss, processes involve events on a small scale, so it is assumed that the specularly reflected plane wave is sampled at some point distant from the actual surface. The reflection loss, *RL*, is an expression in dB of the ratio of the incident intensity to specularly reflected coherent intensity. Some models take account of the size of the insonified patch of sea surface (e.g. Medwin 1966), however this is not considered in this study.

A well-known measure of the acoustical roughness of a surface, which may be applied to the sea surface, is given by the Rayleigh parameter Γ, as

$$\Gamma = \left(4\pi f\, h_\sigma \sin\beta\right)/c_w \qquad (1)$$

where f is cyclic frequency, Hz; h_σ is rms height of the sea surface, metres; β is the acoustic grazing angle with the mean surface plane, radians; c_w is speed of sound in seawater, m/s. For Γ << 1, the sea surface may be considered acoustically smooth, and for Γ >> 1 the surface is considered acoustically rough.

For a sea surface with a Gaussian distribution of surface heights, the well-known Kirchhoff (KA) model of coherent reflection loss (*RL*) for a single surface reflection, in terms of the Rayleigh parameter, is (e.g. Lurton, 2002, section A.3.3)

$$RL = -20\log_{10}\left(e^{-0.5\Gamma^2}\right) \text{ dB per bounce.} \qquad (2)$$

By taking the well-known relation $h_\sigma \approx 5.3\times10^{-3}\left(w_{19.5}\right)^2$ for a Pierson-Moskowitz (PM) surface wave spectrum (e.g. section 13.1 of Medwin and Clay, 1998), where $w_{19.5}$ is wind speed measured 19.5 m above sea level, *RL* for the KA model becomes

$$RL \approx 0.019\left[f\left(w_{19.5}\right)^2 \sin\beta/c_w\right]^2 \text{ dB.} \qquad (3)$$

It is well known that the KA model fails at small grazing angles (e.g. Williams et al. 2004) but it is useful to include it in comparisons against the SSA model, as the latter approaches the KA model for some circumstances, as mentioned in the following section. The reflection loss from the KA model may be seen as simply due to the phase coherent combination of components which are reflected by sections of the sea surface at different heights, for which path length differences, and phase differences, exist. If this model is used to include situations for which the grazing angle of sound at the surface is less than the sea surface slope, it is clear that a problem will exist as part of the surface will be in a shadow, as shown in Figure. 1.

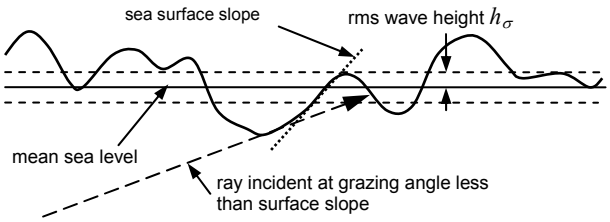

Figure 1. Sound incidence at grazing angle less than surface slope, causing shadowing

The implications of surface shadowing has been considered (e.g. Wagner 1967), although it is by no means certain that this is relevant for roughness scales (wind speeds to 12.5 m/s) and frequencies (1.5 to 9 kHz) of present interest.

Small-slope Model of Reflection Loss

The small-slope approximation model (SSA) considered is the second-order model used and described by Williams et al. (2004) for coherent specular reflection. For high frequencies, this SSA model reverts to the Kirchhoff model (KA), and so does not describe shadowing. The SSA algorithm (Williams et al. (2004) equation 14) has been implemented in this study. In this work it has been established that, for small grazing angles β, this SSA function is

$$RL \approx 3.12\,\alpha\left(k/K_L\right)^{3/2}\beta \text{ dB} \qquad (4)$$

where k is acoustic wave-number in seawater, $K_L = g\sqrt{B}/\left(w_{19.5}\right)^2$ is a surface wave-number expressing a correlation length, $\alpha = 0.0081$ and $B = 0.74$ are parameters of the assumed PM surface wave spectrum and $g = 9.81$ m/s^2 is gravitational acceleration. (It is intended to publish elsewhere full details of the derivation of Equation(4).) Reflection loss is thus a linear function of grazing angle for small angles, becoming

$$RL \approx 2.79\times10^{-7} f^{3/2}\left(w_{19.5}\right)^3\beta \text{ dB} \qquad (5)$$

per bounce in terms of wind speed $w_{19.5}$ and frequency f.

STOCHASTIC MODELLING USING PE

The data presented here are the result of an extension, and some refinement, of a program of stochastic modelling previously described by Jones et al. (2010). Acoustic losses due to scattering at the air-water interface are modelled directly by employing a propagation code which can accommodate an explicitly defined, range-dependent surface profile. The PE model RAMSurf (NRL n.d.) was used, and thus it was assumed that all physical effects including acoustic shadowing of segments of the sea surface and diffraction of sound into shadowed zones were implicitly described. The number of Padé terms used in RAMSurf was three, and presumed adequate. Modelled scenarios depicted a surface duct overlying an isovelocity half-space. The sound speed gradient of each

surface duct was uniform, with different scenarios having different duct depths and gradients.

For each particular combination of source depth and duct configuration, a statistical estimate of scattering loss caused by a particular surface wave spectrum is determined by repeated application of the propagation code, each time using a different and randomly generated realisation of the specified PM wave spectrum. Typically, forty such cycles are used to calculate estimates for both the mean complex acoustic pressure field and the mean acoustic intensity field. A single propagation run with a flat upper-boundary is used to generate reference solutions, i.e. the corresponding fields in the absence of scattering. For this work, the method of generating surface height values at regularly spaced range values is taken from Thorsos (1988) section E, but uses the PM spectrum as described by Williams et al. (2004) equation (8).

For either acoustic parameter, an estimate of the mean perturbation due to scattering at the surface is obtained from the logarithmic difference between corresponding mean and reference fields. This mean perturbation field encodes information on the scattering strength of the surface elevation (wave) spectrum. In practice, the perturbation field is sampled only in those regions of the propagation plane where its spatial variation is relatively low, thus yielding consistent results. Specifically, we interrogate the field along segments of the path of an idealised ray launched horizontally at the source. This reference ray path is generated using BELLHOP (Porter n.d.) for an unperturbed (flat) surface. The surface grazing angle quoted is that of this ray.

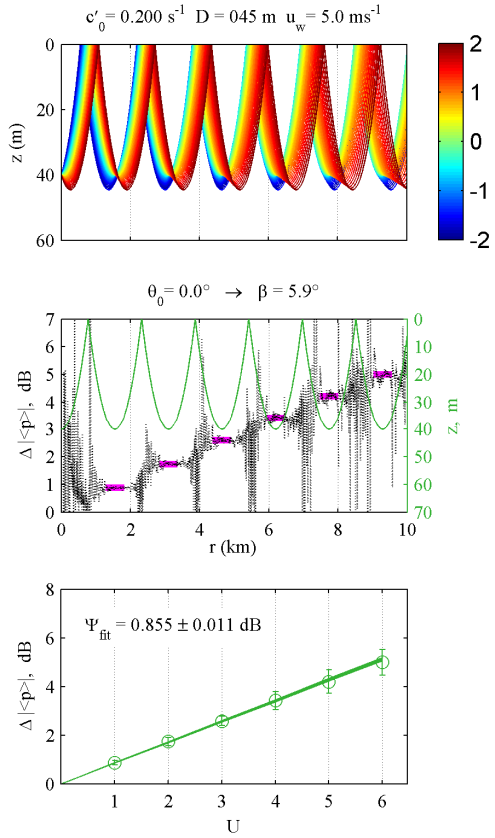

Figure 2. Reflection Loss from stochastic modelling: $w_{19.5}$ = 5 m/s, f = 3.2 kHz, surface incidence angle β = 5.9°

upper: trapped rays at 0.1° increments
centre: loss values along ray launched horizontally
lower: progressive cumulative loss: mean slope (circle), ±2 standard errors (bar) for estimates of slope

A sample extraction of data is shown in Figure 2. Here, the source is relatively deep (40 m) in the surface duct (duct thickness 45 m), so the angular span of trapped rays (upper sub-figure) is not large. The loss data are extracted along the horizontally-launched ray in the region about the refractive turning points, where data are most stable. Values of loss per bounce are determined from the best-fit slope to the cumulative loss (lower sub-figure). Typically, loss per bounce values were found to be similar for each bounce, unless this loss was extremely large and the dynamic range of signal to numerical noise was approached in the PE simulations.

RAMSurf was used to compute the coherent pressure field, across a grid in range r and depth z. One run was executed for each of $k \in \{1, \cdots, n\}$ $(n = 40)$ Monte Carlo realisations of the rough surface in accordance with the appropriate PM spectrum of surface waves. Denoting the coherent pressure p_k at grid point (r, z), we have $p_k = x_k + iy_k$ for the kth surface realisation. The arithmetic mean of the complex pressure values at each grid point, $\left|\left\langle p_{r,z} \right\rangle\right|$, was found as

$$\left|\left\langle p_{r,z} \right\rangle\right| = \frac{1}{n}\sum_{k=1}^{n} x_k + i\frac{1}{n}\sum_{k=1}^{n} y_k \qquad (6)$$

and represents the coherent average, across all surface realisations, of the pressure values at (r, z). In a practical sense, it accounts for the average effect of the reflection from a rough surface, across equivalent but independent surface bounces, when the received signal is processed as coherent pressure. The zero wind, or unperturbed case, was computed with a smooth sea surface. The fluctuating data in the centre sub-figure of Figure 2 show a loss value obtained at relevant (r, z) locations along the path of the ray launched horizontally. These loss data are obtained from the ratio of the $\left|\left\langle p_{r,z} \right\rangle\right|$ values obtained using Equation (6) to the corresponding value obtained from the zero wind case.

Similarly, the mean of the squared pressure values at each grid point, $\left|\left\langle (p_{r,z})^2 \right\rangle\right|$, was determined as

$$\left|\left\langle (p_{r,z})^2 \right\rangle\right| = \frac{1}{n}\sum_{k=1}^{n}\left(x_k{}^2 + y_k{}^2\right) \qquad (7)$$

and represents the energy average, across all surface realisations, of the pressure values at (r, z). The purpose in determining these incoherent or energy data, and in deriving values of energy loss per bounce, is to investigate whether there is any difference with these and the coherent loss per bounce data. This is relevant, as it is common for returns from tonal (continuous wave (CW)), pulses to be processed by a square-law detector (e.g. page 385 Urick (1983)), for which output is proportional to the square of sound pressure input.

COMPARISON OF STOCHASTIC MODELLING WITH SMALL SLOPE APPROXIMATION

Results from this validation, selected to illustrate a range of loss values from very low to very high, are shown below in Figures 3 to 7. For convenience, these are grouped in accordance with wind speeds $w_{19.5}$ of 5, 7.5 and 10 m/s. In each case, values of reflection loss per bounce from the stochastic modelling are compared with the KA and SSA models.

Modelled angles of grazing incidence at the surface, β, ranged from less than 1° to 12°. The circle in each figure identifies the mean loss value for a particular grazing angle, where this was obtained in the stochastic modelling from the mean slope of a cumulative loss, as shown in the lower sub-figure of Figure 2. The span of each bar in each figure represents a spread of ±2 standard errors of the mean loss, and was obtained in the stochastic modelling from the variation in the estimates of the slope of cumulative loss (ref. Figure 2). Data represented in black are the coherent pressure loss values based on $\left|\langle p \rangle\right|$, whereas the data in green represent the energy loss based on $\left|\left\langle p^2 \right\rangle\right|$. For lower loss values, the energy loss was found to coincide with the coherent loss, so energy loss values are shown only for grazing angles for which they differ from the coherent loss. For grazing angles, for particular wind speed/frequency combinations, at which the coherent loss greatly exceeds the energy loss, the specularly reflected energy is then mainly incoherent.

Wind Speed $w_{19.5}$ = 5 ms^{-1}

The data for wind speed $w_{19.5}$ of 5 m/s and frequency 3.2 kHz are shown in Figure 3 for surface grazing angles to 12° (upper sub-figure) and for surface grazing angles to 6° (lower sub-figure). For the span of grazing angles to 12°, each energy loss value was very close to the respective coherent loss value, and is not shown. It is quite evident that the data are all strongly supportive of the SSA model, for all grazing angles shown. At very small grazing angles the data follows the near-linear variation of loss in dB with grazing angle expected from the linear approximation shown earlier.

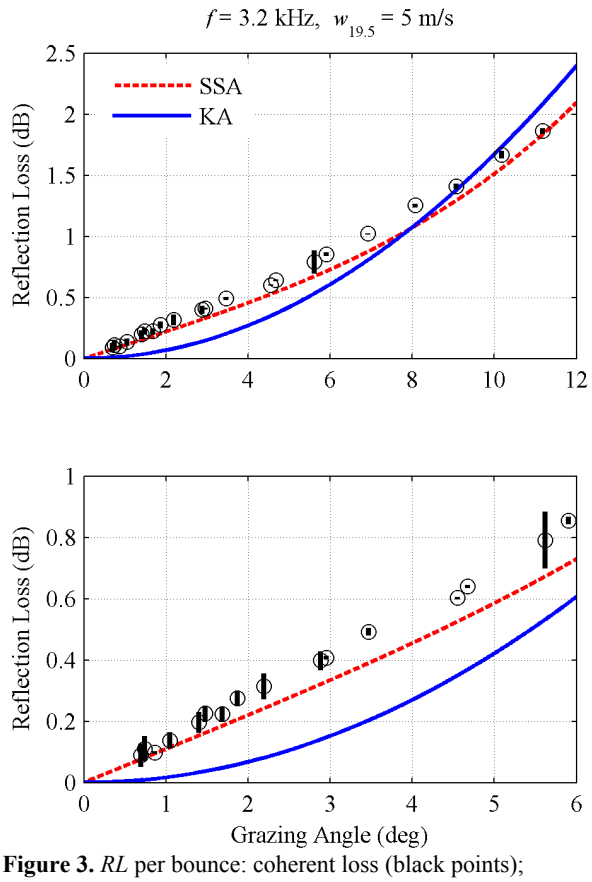

Figure 3. *RL* per bounce: coherent loss (black points); $w_{19.5}$ = 5 m/s, f = 3.2 kHz

Data for wind speed $w_{19.5}$ of 5 m/s and frequency 9 kHz are shown in Figure 4 for surface grazing angles to 12° (upper sub-figure) and for surface grazing angles to 6° (lower sub-figure). Again, the coherent loss data are highly supportive of the SSA model, across the entire range of grazing angles. The energy loss data do not, however, follow the coherent loss data and diverge from the latter at grazing angles of about 8° for which the loss value per bounce is about 6 dB.

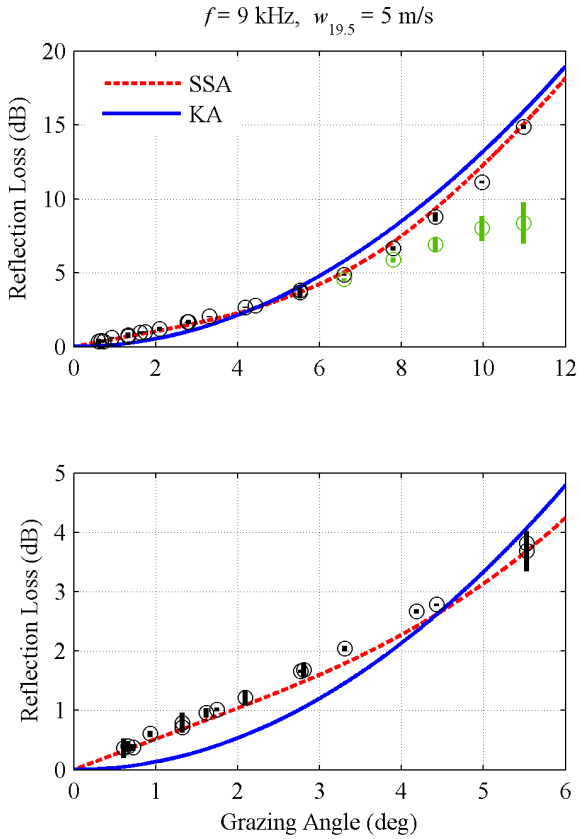

Figure 4. *RL* per bounce: coherent loss (black points), energy loss (green points); $w_{19.5}$ = 5 m/s, f = 9 kHz

Wind Speed $w_{19.5}$ = 7.5 ms^{-1}

The data for wind speed $w_{19.5}$ of 7.5 m/s and frequencies 3.2 kHz and 6 kHz are shown in Figure 5 and Figure 6, respectively, for surface grazing angles to 12° (upper sub-figures) and for surface grazing angles to 6° (lower sub-figures).

Each of Figures 5 and 6 show that the stochastic modelling of coherent loss is highly supportive of the SSA model. For the higher loss scenario in Figure 6, the coherent data show reasonable adherence to SSA up to a loss per bounce of about 28 dB. The agreement is also good at grazing angles as small as 1°, whereas the sea surface slope with 7.5 m/s wind speed is usually much greater than 1°, and shadowing would be expected to be evident. Data in Figure 5 show that the energy-based loss values are close to the coherent loss values, when the loss per bounce is about 5 dB or less, corresponding with grazing angles 8° and less. In Figure 6, the divergence occurs at a similar value of about 5 dB loss per bounce, but this is at a grazing angle of 4.5°. It may be noted that the divergence between energy-based loss values and coherent loss values, as grazing angle is increased, is progressive and not abrupt.

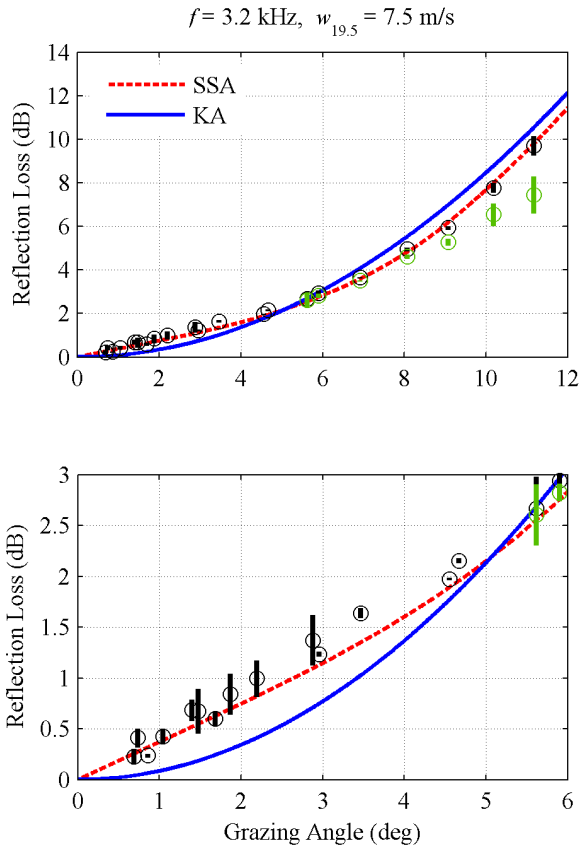

Figure 5. *RL* per bounce: coherent loss (black points), energy loss (green points); $w_{19.5}$ = 7.5 m/s, f = 3.2 kHz

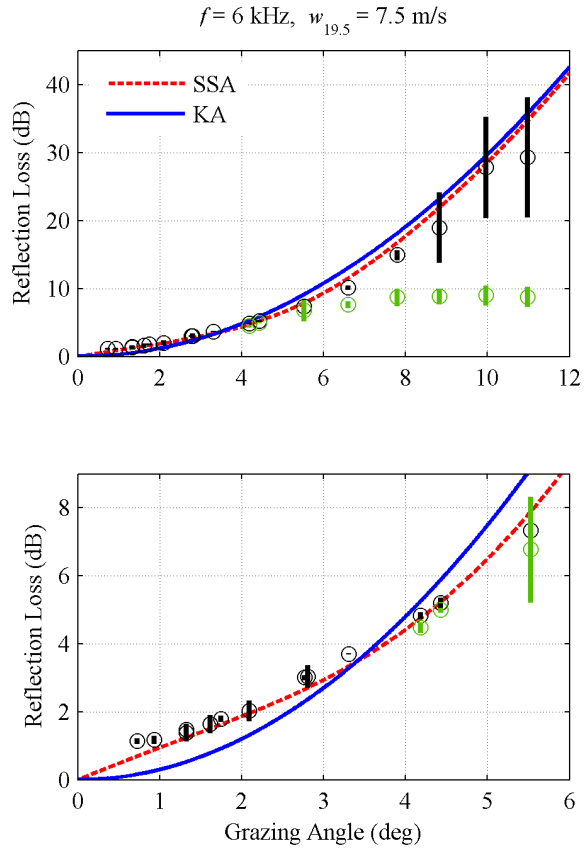

Figure 6. *RL* per bounce: coherent loss (black points), energy loss (green points); $w_{19.5}$ = 7.5 m/s, f = 6 kHz

Wind Speed $w_{19.5}$ = 10 ms^{-1}

The data for wind speed $w_{19.5}$ of 10 m/s and frequency 6 kHz are shown in Figure 7 for surface grazing angles to 12° (upper sub-figure) and for surface grazing angles to 6° (lower sub-figure). These figures show that the coherent loss per bounce follows the SSA model reasonably well for datum points up to and including a grazing angle of 5.6° at which the loss exceeds 20 dB per bounce. The energy loss data, is shown to diverge from the coherent data at a smaller grazing angle. Based on the datum points shown, the divergence is first apparent at a grazing angle of 3.3° at which the loss per bounce is about 7 dB.

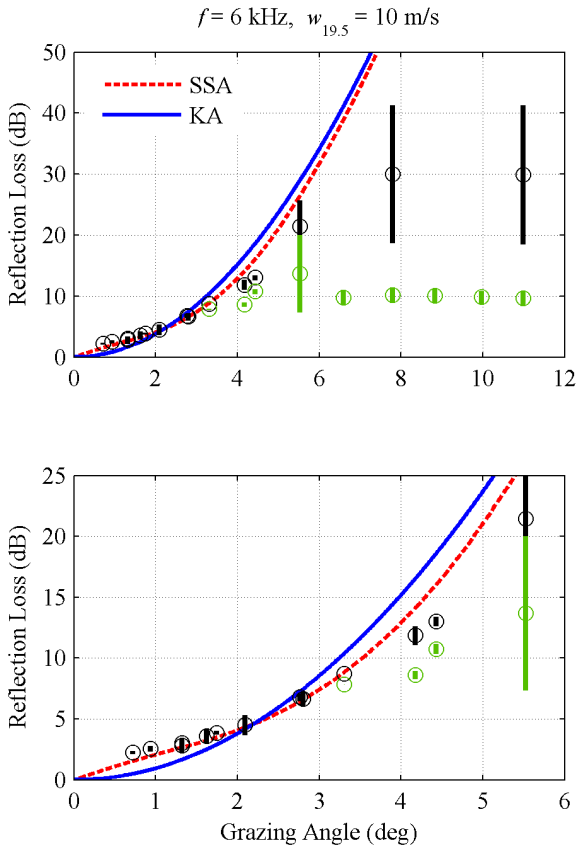

Figure 7. *RL* per bounce: coherent loss (black points), energy loss (green points); $w_{19.5}$ = 10 m/s, f = 6 kHz

DISCUSSION

Each of Figures 3 to 7 shows that the stochastic modelling of coherent loss is highly supportive of the SSA model to values of loss per bounce of up to about 20 dB. The KA model is clearly inadequate at small grazing angles for each case, but for grazing angles steeper than a particular value, does appear to be close to the SSA result. In all cases, the agreement between the coherent and the SSA data is very good at small grazing angles less than 1°, whereas the sea surface slope with wind speeds 7.5 m/s and 10 m/s is usually much greater than 1°, and shadowing would be expected to be evident. Although not shown here, simulations for the very high loss scenario of 9 kHz for a wind speed 12.5 m/s revealed close adherence to the SSA model for grazing angles less than 2°. For this example, the existence of shadowing near the rough surface was confirmed by examining the sound field detail near the wave shapes, using individual stochastic realisations by RAMSurf. Regardless, this shadowing did not appear to result in an observable difference between the SSA model,

which does not describe shadowing phenomena, and the stochastic results. This work suggests that surface shadowing is irrelevant to surface reflection loss for the frequencies studied (9 kHz and less). Note that a more complete description of both the techniques used in this work, and their limitations, and a full set of the results will be submitted for publication elsewhere.

CONCLUSIONS

A stochastic modelling technique, based on Monte Carlo runs of a PE model, has been used in a comparison against the small-slope approximation (SSA) model of coherent reflection loss at the sea surface. A consistent result of this study is that the derived coherent loss per bounce values are highly supportive of the SSA technique for acoustic frequencies to 9 kHz, and for sound incidence angles from less than 1° to at least 12°. For the wind speed and frequency combinations studied, the result from the stochastic modelling is in agreement with the SSA model for coherent loss per bounce values up to about 20 dB. It thus appears that the SSA model may be incorporated within a model of surface reflection loss which incorporates near-surface bubble effects, so long as the appropriate grazing angle, inclusive of refraction due to bubbles, is applied to the SSA model.

This study has shown that the reflection loss per bounce based on mean-square pressure values appears to diverge from loss values based on coherent pressure averages, when the loss per bounce is more than about 5 to 7 dB. This may have consequences for the modelling of detection based on energy processing of CW signal returns.

REFERENCES

Hall, M, V. 1989, 'A comprehensive model of wind-generated bubbles in the ocean and predictions of the effects on sound propagation at frequencies up to 40 kHz', *J. Acoust. Soc. Am.*, vol. 86 (3), pp 1103 – 1117

Jones, A.D., Duncan, A.J., Maggi, A., Clarke, P.A. and Sendt, J. 2010, 'Aspects of practical models of acoustic reflection loss at the ocean surface', *Proceedings of 20th International Congress on Acoustics, ICA 2010*, Sydney, Australia

Jones, A. D., Duncan, A. J., Bartel D. W., Zinoviev, A. and Maggi A. 2011, 'Recent Developments in Modelling Acoustic Reflection Loss at the Rough Ocean Surface', *Proceedings of ACOUSTICS 2011*, Gold Coast, Australia

Kuo, Edward Y. T. 1988, 'Sea Surface Scattering and Propagation Loss: Review, Update and New Predictions', *IEEE J. Oceanic Eng*., vol. 13, No. 4, pp 229 – 234

Lurton, X. 2002, *An Introduction to Underwater Acoustics,* Praxis Publishing Ltd.

Marsh, H. W., Schulkin, M. and Kneale, S. G. 1961, 'Scattering of Underwater Sound by the Sea Surface', *J. Acoust. Soc. Am.*, vol. 33, pp 334 – 340

Medwin, H. 1966, 'Specular Scattering of Underwater Sound from a Wind-Driven Surface', *J. Acoust. Soc. Am.*, vol. 41, pp 1485 – 1495

Medwin, H. and Clay, C.S. 1998, *Fundamentals of Acoustical Oceanography*, Academic Press

NRL n.d., <ftp://ftp.ccs.nrl.navy.mil/pub/ram/RAM/>

Porter, M. B. n.d., 'Ocean Acoustics Library', http://oalib.hlsresearch.com/

Thorsos, E. I. and Broschat, S. L. 1995, 'An investigation of the small slope approximation for scattering from rough surfaces. Part I. Theory', *J. Acoust. Soc. Am.*, vol. 97, pp 2082 – 2093

Thorsos, E. I. 1988, 'The validity of the Kirchhoff approximation for rough surface scattering using a Gaussian roughness spectrum', *J. Acoust. Soc. Am.*, vol. 83, pp 78 – 92

Urick, R.J. 1983, *Principles of Underwater Sound*, 3rd edition, Peninsula Publishing, Los Altos

Wagner, R. J. 1967, 'Shadowing of Randomly Rough Surfaces', *J. Acoust. Soc. Am.*, vol. 41, no. 1, pp 138 – 147

Williams, K. L., Thorsos, E. I. and Elam, W. T. 2004, 'Examination of coherent surface reflection coefficient (CSRC) approximations in shallow water propagation', *J. Acoust. Soc. Am.*, vol. 116, no. 4, pp 1975 – 1984